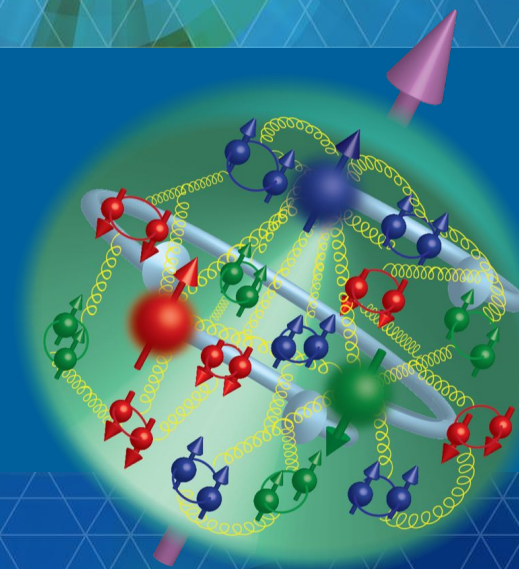


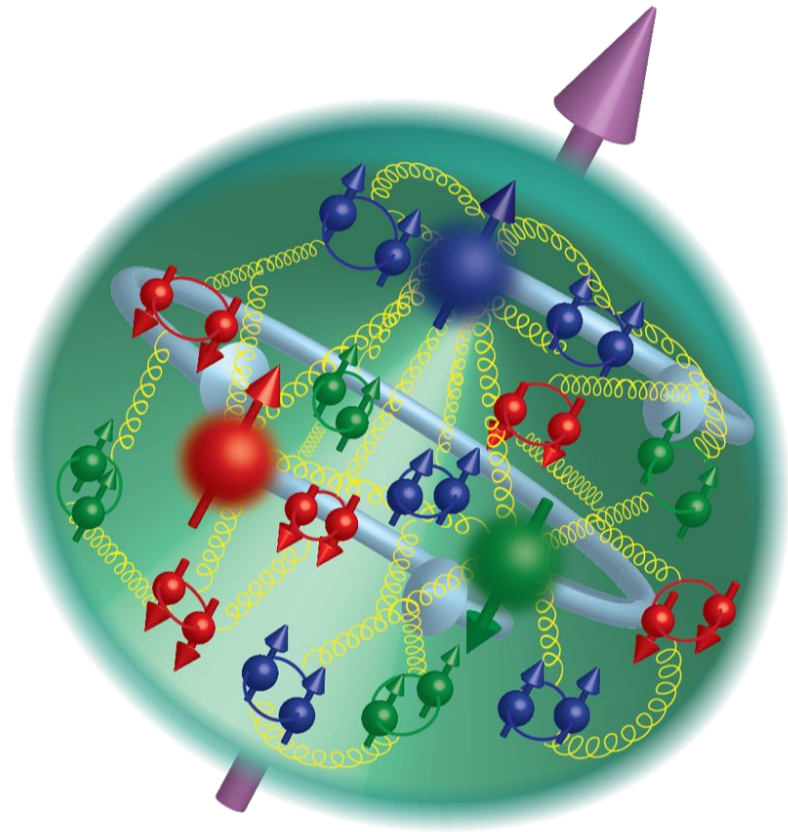
2nd workshop on advancing the understanding of non-perturbative QCD using energy flow

Stony Brook University, 6-9 November, 2023

Overview of 3D structure results at CLAS12



Maria ŻUREK
Argonne National Laboratory, zurek@anl.gov



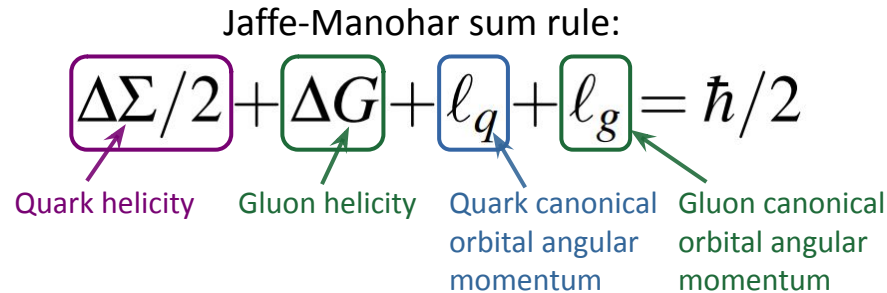
Physics Question

How does the **spin of the nucleon originate** from its **quark, anti-quark, and gluon** constituents and their dynamics?

Jaffe-Manohar sum rule:

$$\Delta\Sigma/2 + \Delta G + \ell_q + \ell_g = \hbar/2$$

Quark helicity Gluon helicity Quark canonical orbital angular momentum Gluon canonical orbital angular momentum



- All terms have **partonic interpretation**
- In infinite-momentum frame
- **ℓ_q and ℓ_g** (Twist-3 quantities) can be extracted **from GPDs**
- Nucl. Phys. B 337, 509–546 (1990)

Physics Questions

How is the **nucleon spin correlated with the motion** of quarks and gluons?

How is the **nucleon spin correlated with the spatial distribution** of partons?

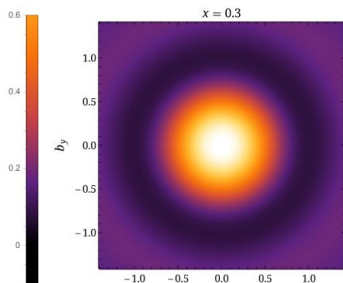
Nucleon tomography

Impact parameter dependent

parton distribution functions $f(x, b_T)$

Can be accessed from **GPDs**: $H(x, \xi, t) \rightarrow f(x, b_T)$

- Extrapolation to zero skewness $\xi \rightarrow 0$
- Fourier Transformation $t \leftrightarrow b_T$

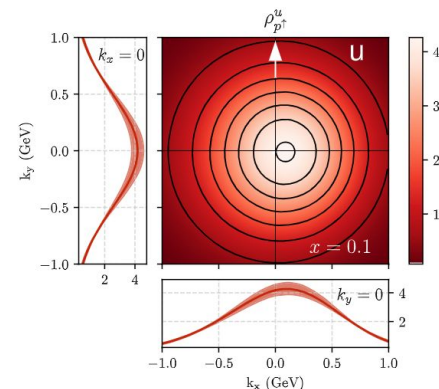


Huey-Wen Lin, PRL 127 (2021) 18, 182001, from Lattice

Position space

Transverse momentum dependent

parton distribution functions (TMDs) $f(x, k_T)$



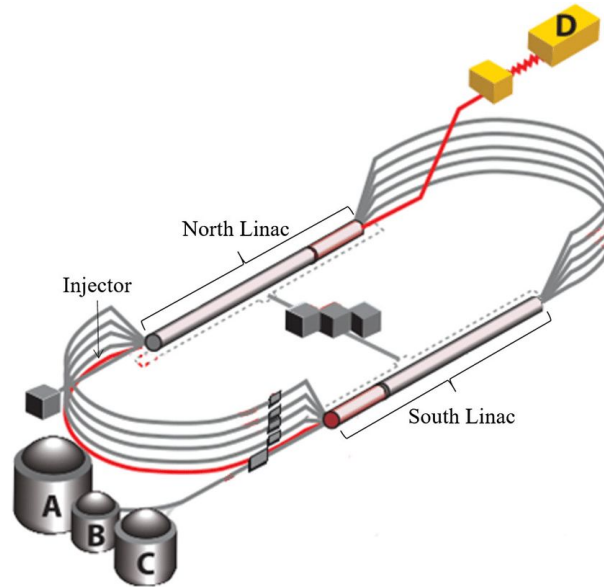
A. Bacchetta, F. Delcarro, C. Pisano, M. Radici, PLB 827 (2022) 136961, from SIDIS and DY/W data

Momentum space

CLAS12

The image features a vibrant green background with a complex, layered pattern of overlapping circles and squares. A bright, glowing yellow-green circular area is positioned in the upper right quadrant, radiating light. At the bottom of the image, there is a horizontal band with a white grid pattern of intersecting lines forming a series of 'X' shapes.

Thomas Jefferson National Accelerator Facility



Continuous Electron Beam Accelerator Facility (CEBAF)

- 12 GeV continuous polarized electron beam
- Four experimental halls: A, B, C, D

CLAS12 located in Hall B
high luminosity, wide acceptance

Began data taking in Spring 2018

- 2018-2020: unpolarized proton/deuterium target
- 2022/23 longitudinally polarized proton/deuterium target ~5 % produced

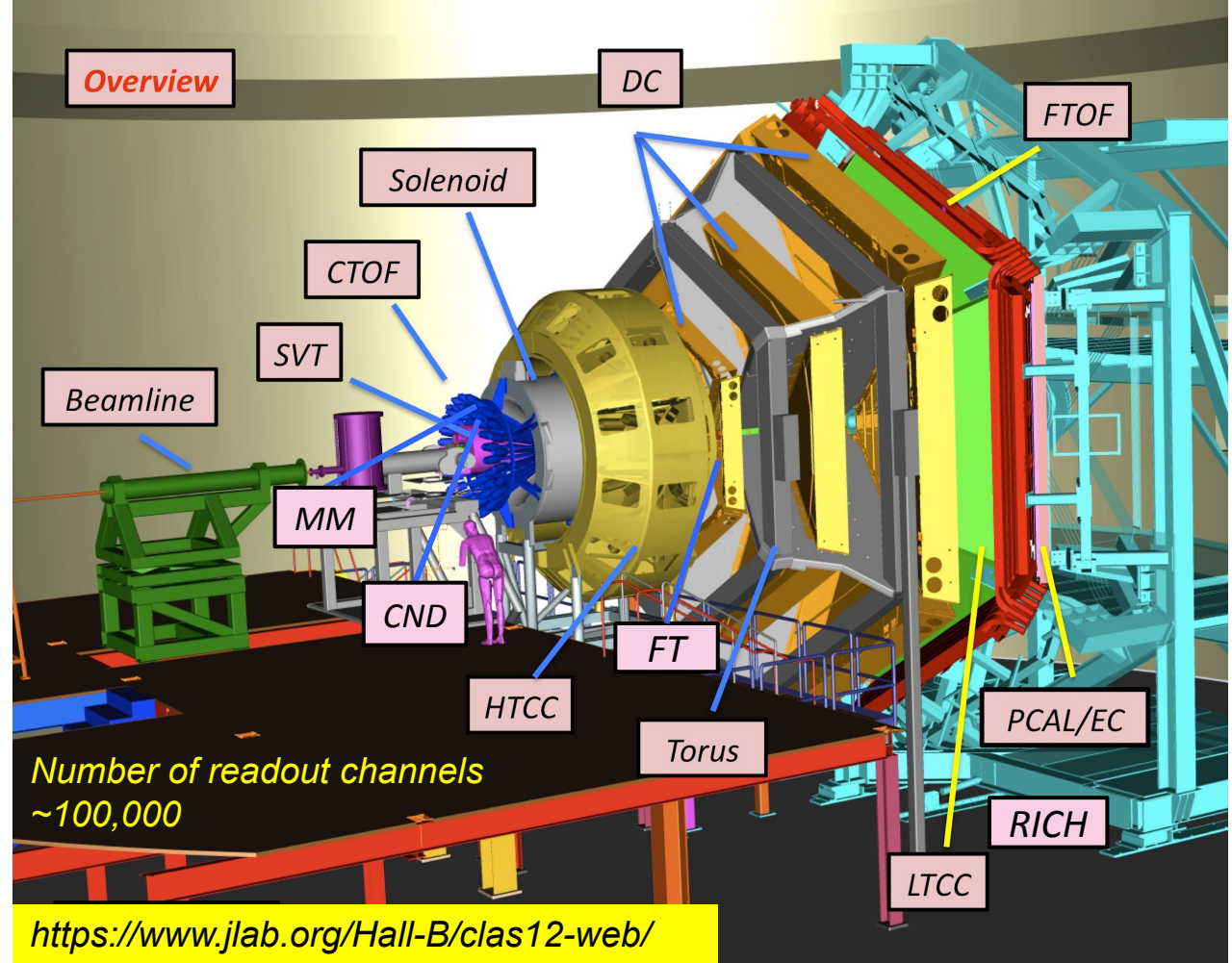


Forward Detector:

- TORUS magnet
- HT Cherenkov Counter
- Drift chamber system
- LT Cherenkov Counter
- Forward ToF System
- Preshower calorimeter
- EM calorimeter (EC)
- RICH detector
- Forward Tagger

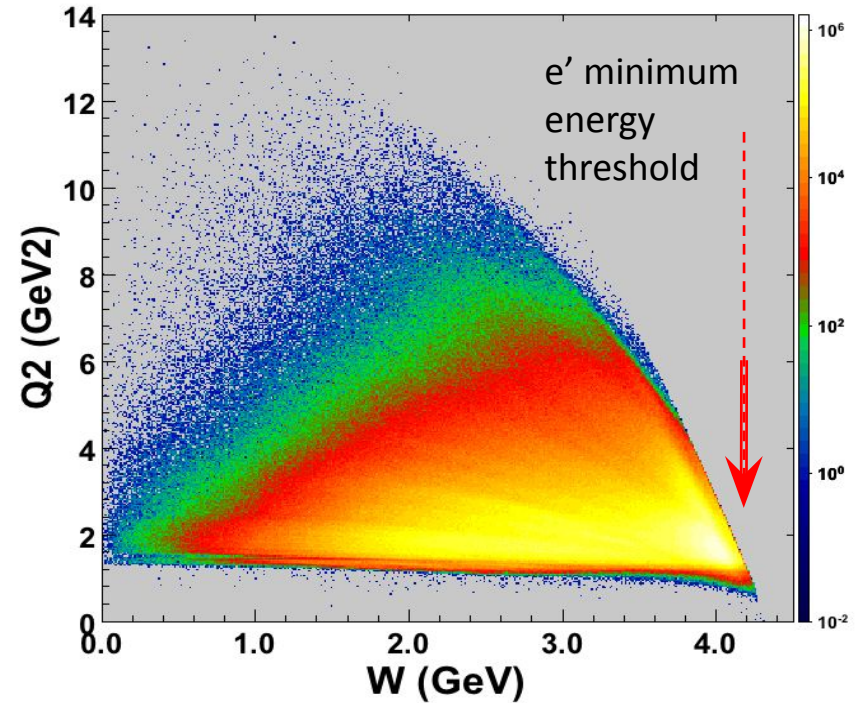
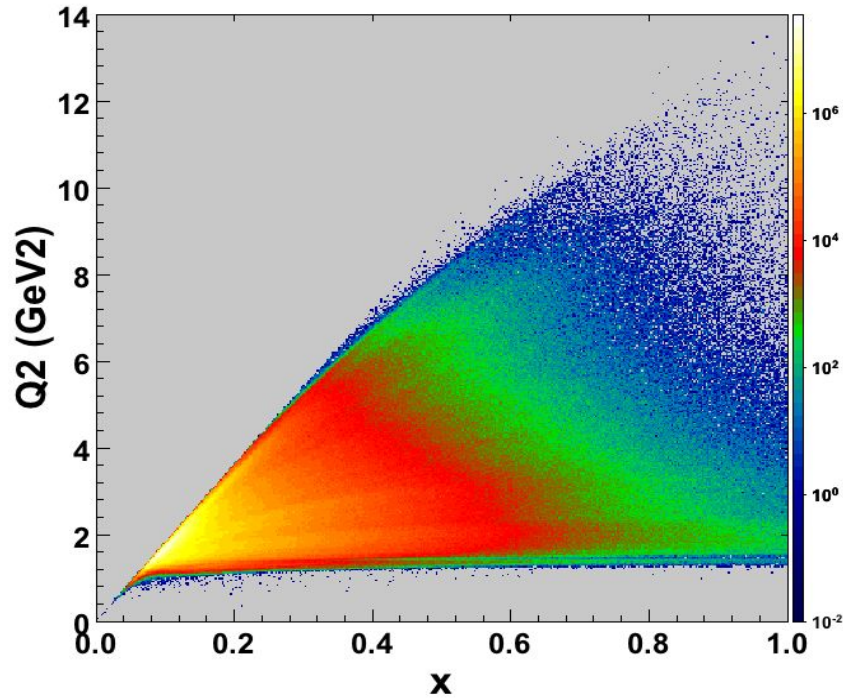
Central Detector:

- Solenoid magnet
- Barrel Silicon Tracker
- Central Time-of-Flight
- Central Neutron Detector
- Micromegas Tracker



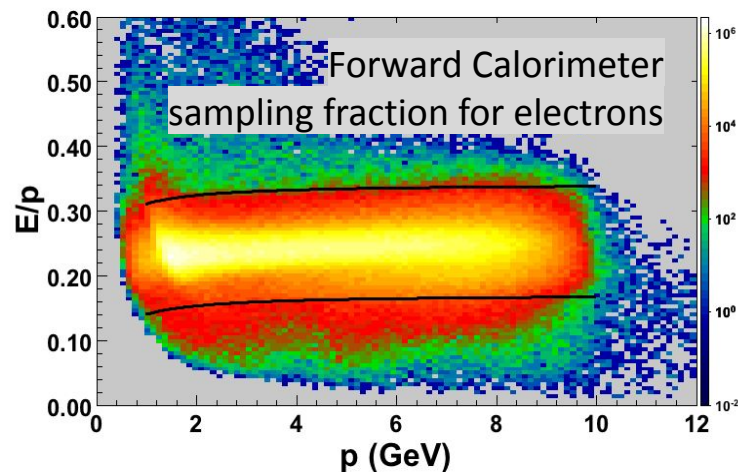
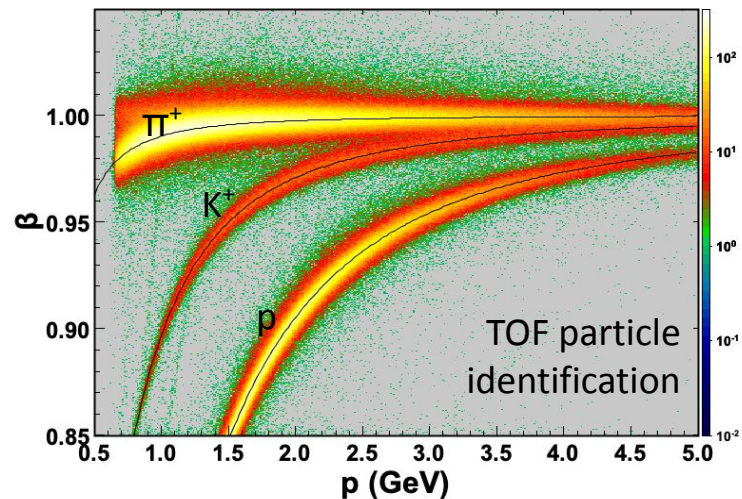
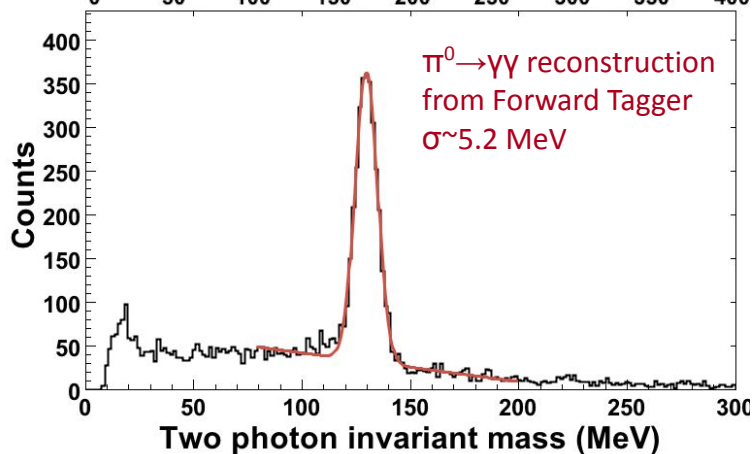
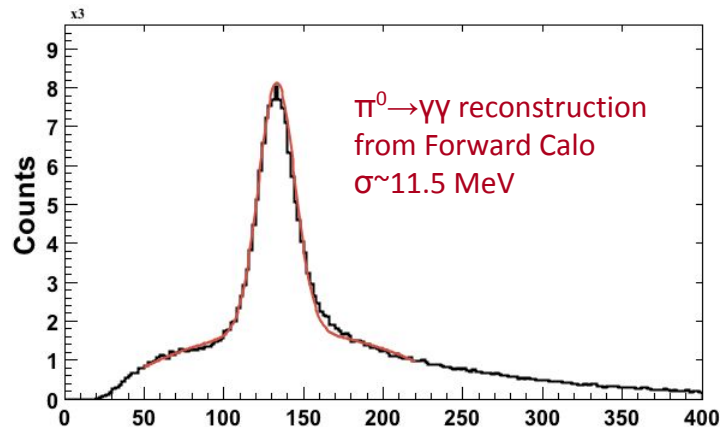
CLAS12 Kinematic Reach

$p(e,e')X$, plots based on 200 min. of data taking



Beam energy at 10.6 GeV Torus current 3770 A, electrons in-bending, Solenoid magnet at 2416 A.

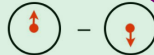
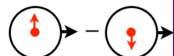
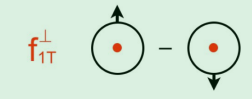
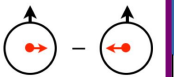
CLAS12 Particle ID



The background features a green-to-yellow gradient with a circular radar-like pattern of concentric arcs and radial lines. At the bottom, there is a dark green horizontal band with a white grid of intersecting lines.

Selected TMD results

TMDs and Spin-Orbit Correlations

		Quark Polarization		
		U	L	T
Nucleon Polarization	U	f_1  unpolarized		h_1^\perp  Boer-Mulders
	L		g_{1L}  helicity	h_{1L}^\perp  longi-transversity (worm-gear)
	T	f_{1T}^\perp  Sivers	g_{1T}  trans-helicity (worm-gear)	h_1  transversity h_{1T}^\perp  pretzelosity

TMDs surviving integration over k_T

Naive time-reversal odd TMDs describing strength of **spin-orbit correlations**

Chiral odd TMDs

Off-diagonal part vanishes without parton's transverse motion

TMDs describing strength of spin-orbit correlations non-zero → indication of parton OAM

- No quantitative relation between TMDs & OAM identified yet
- **Sivers**: correlations of transverse-spin direction and the parton transverse momentum
- **Boer-Mulders**: correlations of parton transverse spin and parton transverse momentum
- **Collins**: fragmentation of a transversely polarized parton into a final-state hadron

Access to TMDs from the SIDIS Cross Section

Unpolarized and Longitudinally Polarized Targets

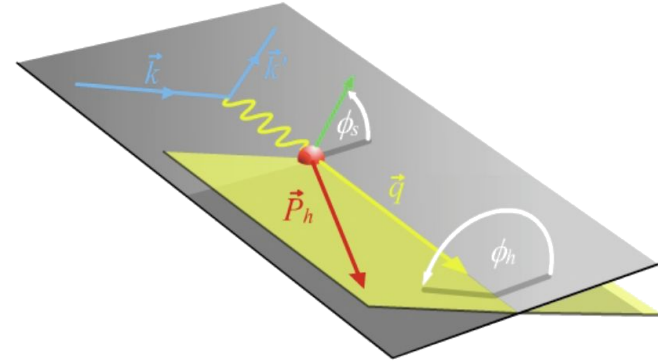
$$\frac{d^6\sigma}{dx dy d\psi dz d\phi_h dP_T^2} = \frac{\alpha^2}{xyQ^2} \frac{y^2}{2(1-\varepsilon)} \left(1 + \frac{\gamma^2}{2x}\right) \cdot$$

$$\left\{ F_{UU,T} + \varepsilon F_{UU,L} + \sqrt{2\varepsilon(1+\varepsilon)} F_{UU}^{\cos\phi_h} \cos\phi_h + \varepsilon F_{UU}^{\cos 2\phi_h} \cos 2\phi_h \right.$$

$$+ \lambda \left(\sqrt{2\varepsilon(1-\varepsilon)} F_{LU}^{\sin\phi_h} \sin\phi_h \right)$$

$$+ S_L \left(\sqrt{2\varepsilon(1+\varepsilon)} F_{UL}^{\sin\phi_h} \sin\phi_h + \varepsilon F_{UL}^{\sin 2\phi_h} \sin 2\phi_h \right)$$

$$+ S_L \lambda \left(\sqrt{1-\varepsilon^2} F_{LL} + \sqrt{2\varepsilon(1-\varepsilon)} F_{LL}^{\cos\phi_h} \cos\phi_h \right)$$



Leading twist formalism
(higher-twist terms can be included)

$$F_{UU,T} = C [f_1 D_1]$$

$$F_{UU}^{\cos 2\phi_h} = C \left[\frac{2(\hat{h} \cdot k_T)(\hat{h} \cdot p_\perp) - k_T \cdot p_\perp}{zMM_h} h_1^\perp H_1^\perp \right]$$

$$F_{UL}^{\sin 2\phi_h} = C \left[\frac{2(\hat{h} \cdot k_T)(\hat{h} \cdot p_\perp) - k_T \cdot p_\perp}{zMM_h} h_{1L}^\perp H_1^\perp \right]$$

$$F_{LL} = C [g_{1L} D_1]$$

Unpolarized PDF \otimes Unpolarized fragmentation function

Boer-Mulders \otimes Collins Fragmentation Function

Worm-gear \otimes Collins Fragmentation Function

Helicity \otimes Unpolarized fragmentation function

Access to TMDs from the SIDIS Cross Section

Transversely Polarized Target

$$\frac{d^6\sigma}{dx dy d\psi dz d\phi_h dP_T^2} = \frac{\alpha^2}{xyQ^2} \frac{y^2}{2(1-\epsilon)} \left(1 + \frac{\gamma^2}{2x}\right).$$

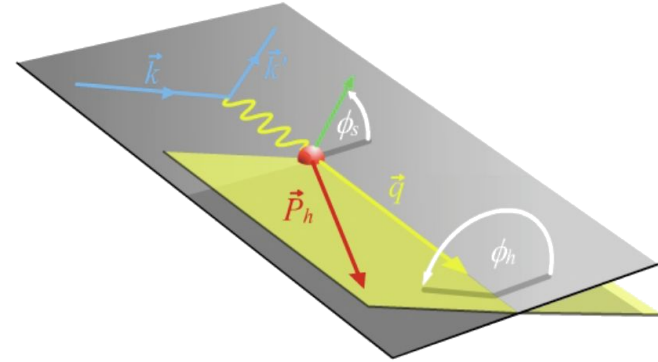
$$\left\{ \begin{aligned} & S_T \left(\left(F_{UT,T}^{\sin(\phi_h - \phi_S)} + \epsilon F_{UT,L}^{\sin(\phi_h - \phi_S)} \right) \sin(\phi_h - \phi_S) \right. \\ & \quad + \epsilon F_{UT}^{\sin(\phi_h + \phi_S)} \sin(\phi_h + \phi_S) + \epsilon F_{UT}^{\sin(3\phi_h - \phi_S)} \sin(3\phi_h - \phi_S) \\ & \quad \left. + \sqrt{2\epsilon(1+\epsilon)} F_{UT}^{\sin\phi_S} \sin\phi_S + \sqrt{2\epsilon(1+\epsilon)} F_{UT}^{\sin(2\phi_h - \phi_S)} \sin(2\phi_h - \phi_S) \right) \\ & + S_T \lambda \left(\sqrt{1-\epsilon^2} F_{LT}^{\cos(\phi_h - \phi_S)} \cos(\phi_h - \phi_S) \right. \\ & \quad \left. + \sqrt{2\epsilon(1-\epsilon)} F_{LT}^{\cos\phi_S} \cos\phi_S + \sqrt{2\epsilon(1-\epsilon)} F_{LT}^{\cos(2\phi_h - \phi_S)} \cos(2\phi_h - \phi_S) \right) \end{aligned} \right\}$$

$$F_{UT,T}^{\sin(\phi_h - \phi_S)} = C \left[-\frac{\hat{h} \cdot \mathbf{k}_T}{M} f_{1T}^\perp D_1 \right]$$

$$F_{UT}^{\sin(\phi_h + \phi_S)} = C \left[\frac{\hat{h} \cdot \mathbf{p}_\perp}{zM_h} h_1 H_1^\perp \right]$$

$$F_{UT}^{\sin(3\phi_h - \phi_S)} = C \left[-\frac{2(\hat{h} \cdot \mathbf{k}_T)(\mathbf{k}_T \cdot \mathbf{p}_\perp) + k_T^2(\hat{h} \cdot \mathbf{p}_\perp) - 4(\hat{h} \cdot \mathbf{k}_T)^2(\hat{h} \cdot \mathbf{p}_\perp)}{2zM_h^2 M_h} h_{1T}^\perp H_1^\perp \right]$$

$$F_{LT}^{\cos(\phi_h - \phi_S)} = C \left[\frac{\hat{h} \cdot \mathbf{k}_T}{M} g_{1T} D_1 \right]$$



Leading twist formalism
(higher-twist terms can be included)

Sivers \otimes Unpolarized fragmentation function

Transversity \otimes Collins Fragmentation Function

Pretzelosity \otimes Collins Fragmentation Function

Worm Gear \otimes Unpolarized fragmentation function

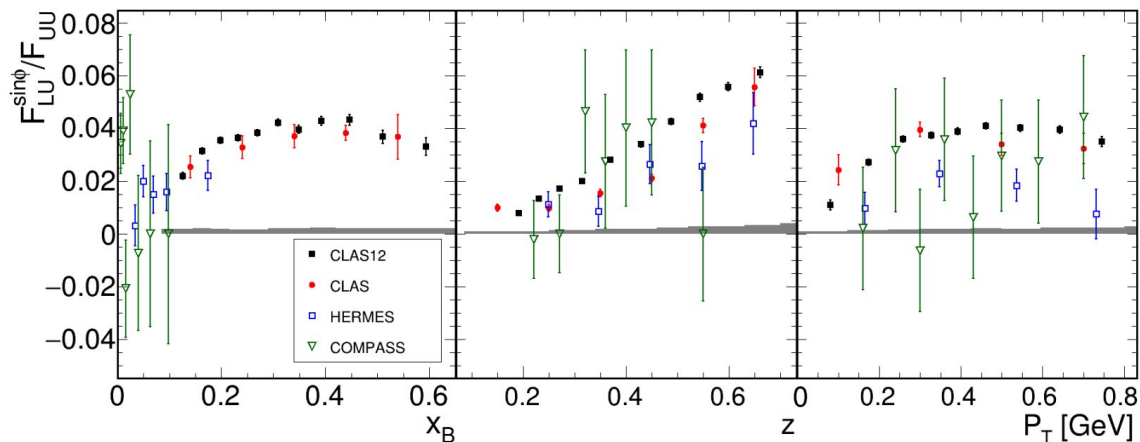
Single Pion Beam Spin Asymmetries

$$F_{LU}^{\sin\phi_h} = \frac{2M}{Q} \mathcal{C} \left[-\frac{\hat{h} \cdot k_T}{M_h} \left(x e H_1^\perp + \frac{M_h}{M} f_1 \frac{\tilde{G}^\perp}{z} \right) + \frac{\hat{h} \cdot p_T}{M} \left(x g^\perp D_1 + \frac{M_h}{M} h_1^\perp \frac{\tilde{E}}{z} \right) \right]$$

twist-3 pdf unpolarized PDF twist-3 t-odd PDF Boer-Mulders
Collins FF twist-3 FF unpolarized FF twist-3 FF

N/q	U	L	T
U	f^\perp	g^\perp	h, e
L	f_L^\perp	g_L^\perp	h_L, e_L
T	f_T, f_T^\perp	g_T, g_T^\perp	$h_T, e_T, h_T^\perp, e_T^\perp$

CLAS12, S. Diehl et al., Phys. Rev. Lett., 128, 062005, (2022), [hep:ex] 2101.03544



Multidimensional analysis performed

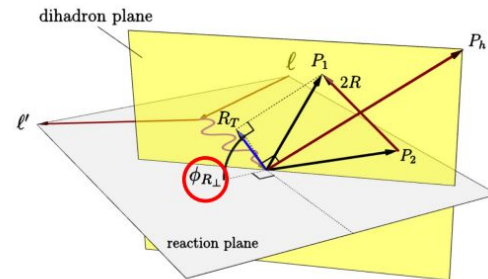
Data sensitive to the eH_1^\perp (DCSB) and $g^\perp D_1$ (quark gluon correlation)

For single-pion SIDIS - $e(x)$ is accessible only when the transverse momentum of the final hadron is not integrated out

Di-hadron Beam Spin Asymmetries

$$F_{LU}^{\sin \phi_{R\perp}} = -x \frac{\vec{R} \sin \theta}{Q} \left[\frac{M}{M_h} x e^q(x) \overset{\text{twist-3 pdf}}{H_1^{\leq q}(z, \cos \theta, M_h)} + \frac{1}{z} \overset{\text{unpolarized pdf}}{f_1^q(x)} \overset{\text{twist-3 FF}}{\tilde{G}(z, \cos \theta, M_h)} \right]$$

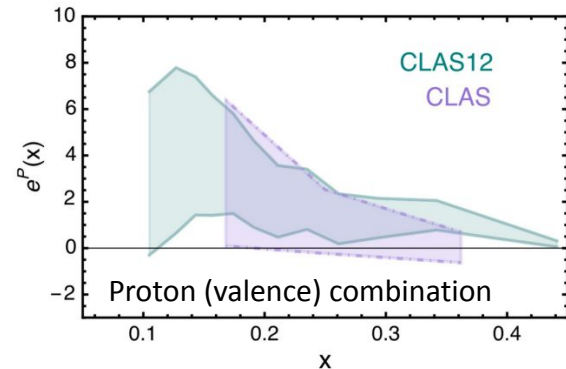
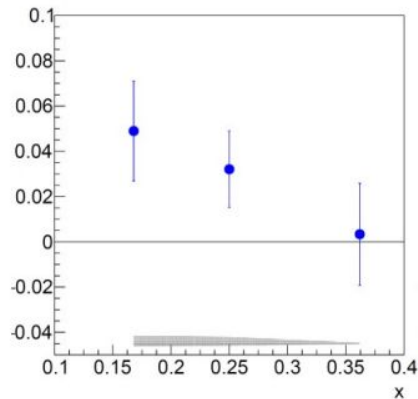
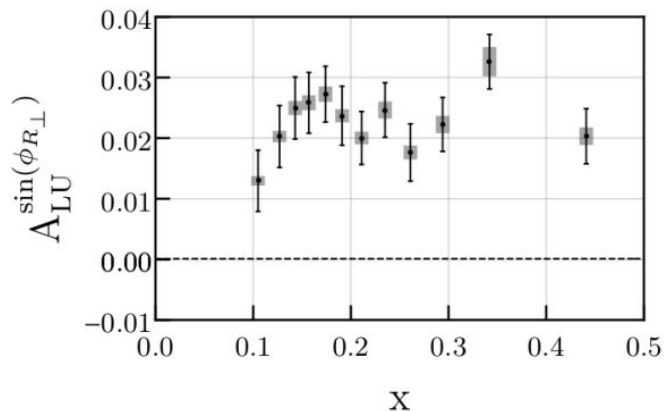
“Interference Fragmentation Function”
twist-3 FF



CLAS12, T. Hayward, et al., PRL 126 (2021) 152501

CLAS6, M. Mirazita, et al., PRL 126 (2021) 6, 062002

A. Courtoy, et al., Phys.Rev.D 106 (2022) 1, 014027

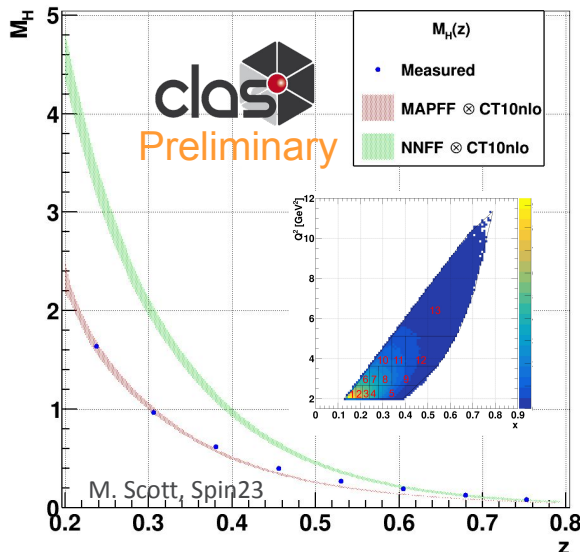


- First measurement of dihadron A_{LU} and extraction of $e(x)$: IFF measured at Belle combined with CLAS results
- Twist-3 PDF (quark gluon correlations): related to quark contributions to nucleon mass
- Boer-Mulders force: \perp force exerted by color field on a \perp polarized struck quark in an unpolarized nucleon

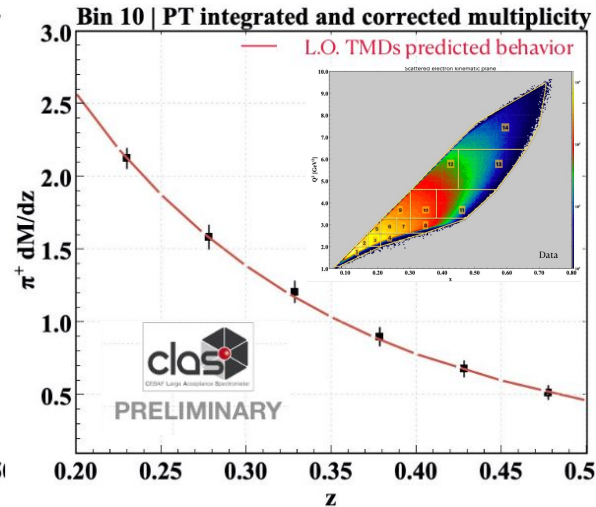
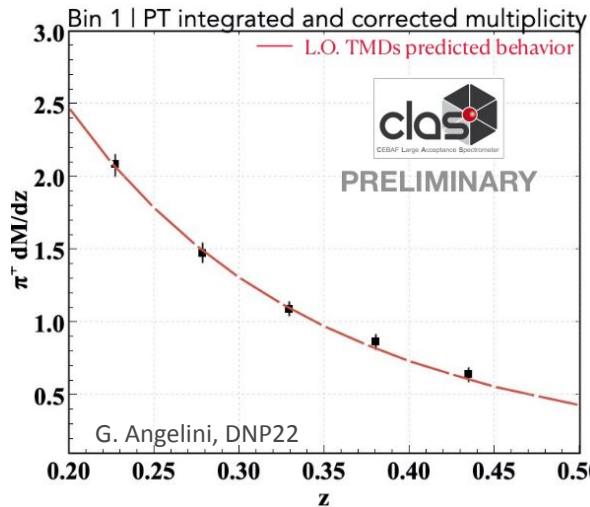
Pion Multiplicities

- Pion multiplicities describe the number of produced pions in the five-dimensional SIDIS phase space $(x, Q^2, z, p_T^2, \Phi_h)$ per number of DIS events in (x, Q^2) phase space.
- Directly related to the $D_1(z)$ FF $m_N^h(x, z, P_{hT}^2) = \frac{\pi}{\sum_a e_a^2 f_1^a(x)} \sum_a e_a^2 f_1^a(x) D_1^{a \rightarrow h}(z) \frac{e^{-P_{hT}^2 / (z^2 \langle k_{\perp,a}^2 \rangle + \langle P_{\perp,a \rightarrow h}^2 \rangle)}}{\pi(z^2 \langle k_{\perp,a}^2 \rangle + \langle P_{\perp,a \rightarrow h}^2 \rangle)}$
- Neutral pion results further serve as a test on the isospin symmetry between neutral and charged pion FF

Example p_T^2 integrated π^0 multiplicity for x - Q^2 Bin 1 with LO 1σ theory curves



Example p_T^2 integrated π^+ multiplicity for x - Q^2 Bin 1 and 10 with LO theory curves (CTEQ and Sassot)

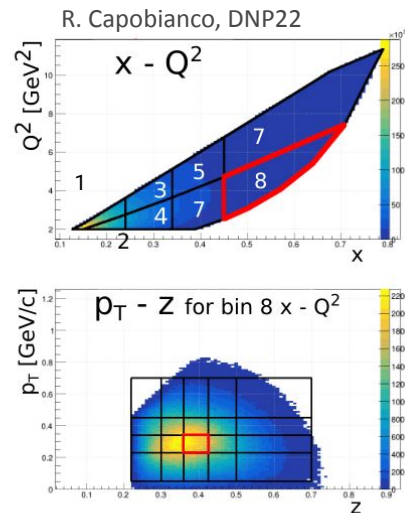
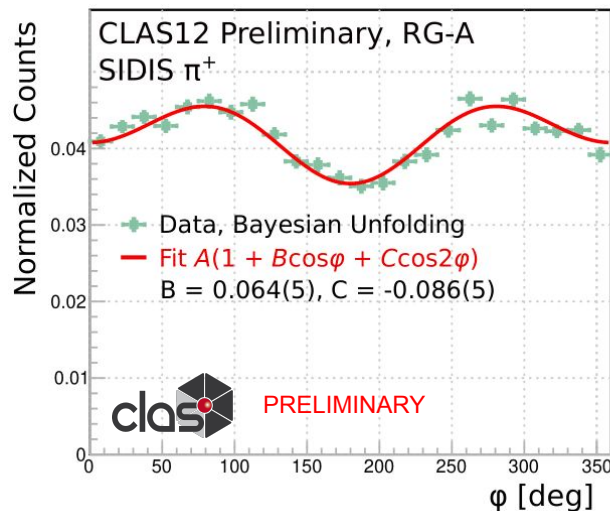


Cos φ_h and Cos2 φ_h Moments of the SIDIS cross section

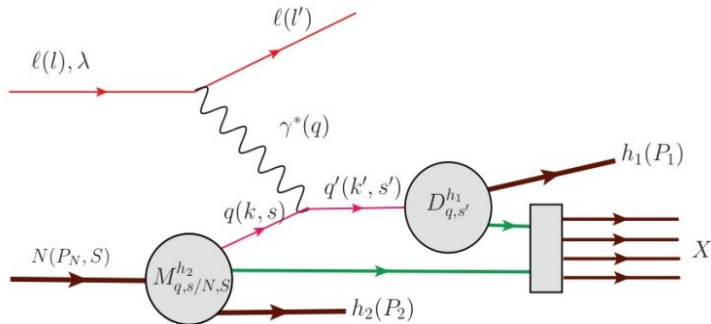
- $\cos(\varphi_h)$ and $\cos(2\varphi_h)$ moments of unpolarized SIDIS cross-section for π^+ using hydrogen target
- High-precision study of the moments which probe the Boer-Mulders function and Cahn effect
- The high-statistics data will, for the first time, enable a multidimensional analysis over a large kinematic range of Q^2 , y , z , and P_T .

Structure functions connection to Boer-Mulders and Cahn effects:

$$\begin{aligned}
 & \text{leading twist} \\
 & F_{UU}^{\cos 2\varphi_h} \propto C \left[\frac{2(\vec{P}_{h\perp} \cdot \vec{k}_T)(\vec{P}_{h\perp} \cdot \vec{p}_T) - \vec{k}_T \cdot \vec{p}_T}{MM_h} \frac{1}{h_1^\perp H_1^\perp} + \dots \right] \quad \begin{array}{l} \text{BOER-MULDERS} \\ \text{EFFECT} \end{array} \\
 & \text{next to leading twist} \\
 & F_{UU}^{\cos \varphi_h} \propto \frac{2M}{Q} C \left[\frac{-\vec{P}_{h\perp} \cdot \vec{k}_T}{M_h} x h H_1^\perp - \frac{\vec{P}_{h\perp} \cdot \vec{p}_T}{M} f_1 D_1 + \dots \right] \quad \begin{array}{l} \text{CAHN EFFECT} \\ \text{Interaction dependent} \\ \text{terms neglected} \end{array}
 \end{aligned}$$



Current and Target Fragmentation Region Correlations

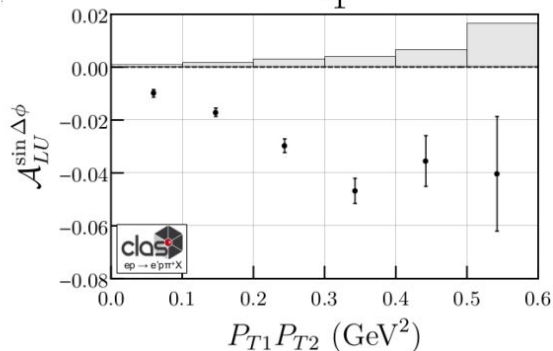


- Fracture functions accessible in “Back-to-Back” production
- One current-fragmentation region (CFR) hadron h_1
 - One target-fragmentation region (TFR) hadron h_2

Fracture functions: the probability for the target remnant to form a certain hadron given a particular ejected quark

CLAS12, H. Avakian, et al., Phys.Rev.Lett. 130 (2023) 2, 022501

CFR pion, TFR proton $\rightarrow \hat{I}_1^{\perp P}$ (L quark, U nucleon)
 $\rightarrow \hat{U}_1^P$ (unpolarized)



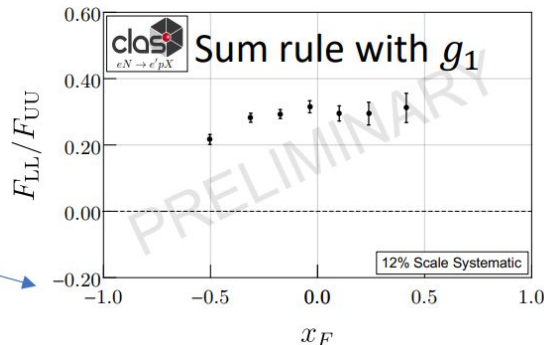
CLAS12 Preliminary, T. Hayward, Spin23

Quark polarization

	U	L	T
U	\hat{u}_1	$\hat{I}_1^{\perp h}$	$\hat{I}_1^h, \hat{I}_1^\perp$
L	$\hat{u}_{1L}^{\perp h}$	\hat{I}_{1L}^h	$\hat{I}_{1L}^h, \hat{I}_{1L}^\perp$
T	$\hat{u}_{1T}^h, \hat{u}_{1T}^\perp$	$\hat{I}_{1T}^h, \hat{I}_{1T}^\perp$	$\hat{I}_{1T}^h, \hat{I}_{1T}^{\perp h}$ $\hat{I}_{1T}^\perp, \hat{I}_{1T}^{\perp h}$

Nucleon polarization

M. Anselmino et al., Phys. Lett. B. 706 (2011), 46-52, [hep-ph/1109.1132]





Selected GPD results

GPDs and Angular Orbital Momentum

Connection to the **proton spin**: $J_q = \frac{1}{2} \lim_{t \rightarrow 0} \int_{-1}^1 dx x [H^q(x, \xi, t) + E^q(x, \xi, t)]$ $J_q = \frac{1}{2} \Delta \Sigma + L_q$

N/q	U	L	T
U	H		E_T
L		\tilde{H}	\tilde{E}_T
T	E	\tilde{E}	$H_T \tilde{H}_T$

4 chiral-even and 4 chiral-odd quark **GPDs at leading twist** for a spin- $\frac{1}{2}$ hadron

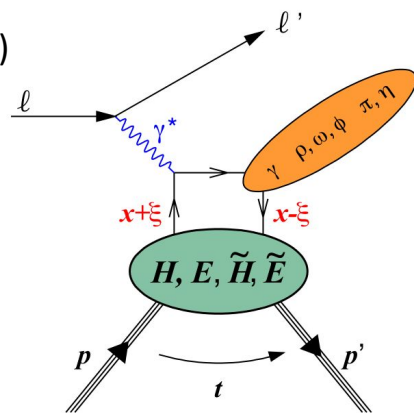
Accessed via hard exclusive processes: cross section and asymmetries

- Deep virtual Compton scattering (**DVCS**) and hard exclusive meson production (**HEMP**)
- H, E accessed in vector meson production, all 4 chiral-even GPDs accessed in DVCS

DVCS and access to GPDs

- Experimental access to GPDs via Compton Form Factors
- Different configurations: p and e polarization, beam charge \rightarrow different CFFs
- proton + neutron DVCS \rightarrow flavor separation of GPDs

$$\mathcal{H}(\xi, t) = \sum_q e_q^2 \int_{-1}^1 dx H^q(x, \xi, t) \left(\frac{1}{\xi - x - i\epsilon} - \frac{1}{\xi + x - i\epsilon} \right)$$



GPDs and Angular Orbital Momentum

Connection to the **proton spin**: $J_q = \frac{1}{2} \lim_{t \rightarrow 0} \int_{-1}^1 dx x [H^q(x, \xi, t) + E^q(x, \xi, t)]$ $J_q = \frac{1}{2} \Delta \Sigma + L_q$

N/q	U	L	T
U	H		E_T
L		\tilde{H}	\tilde{E}_T
T	E	\tilde{E}	$H_T \tilde{H}_T$

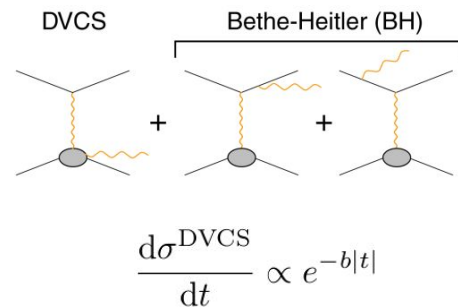
4 chiral-even and 4 chiral-odd quark **GPDs at leading twist** for a spin- $\frac{1}{2}$ hadron

Interference between DVCS and Bethe-Heitler amplitude plays key role

- Allows to determine both magnitude and phase of the DVCS amplitude

$$\sigma = |\mathcal{T}_{\text{DVCS}}|^2 + (\mathcal{T}_{\text{DVCS}} \mathcal{T}_{\text{BH}} + \mathcal{T}_{\text{DVCS}} \mathcal{T}_{\text{BH}}) + |\mathcal{T}_{\text{BH}}|^2$$

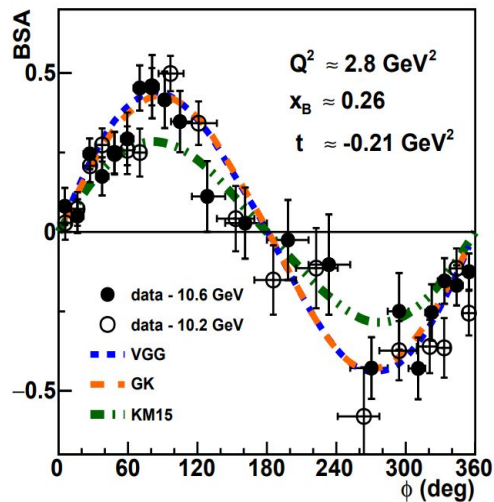
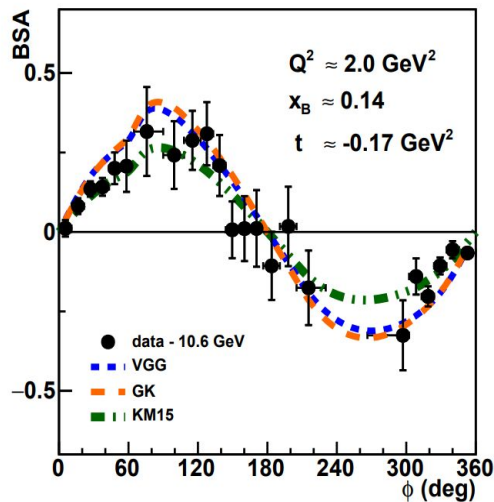
Slope of DVCS $d\sigma/dt$ - determination of **transverse extension of partons**



DVCS AND TCS AT CLAS12

G. Christiaens et al. (CLAS), Phys. Rev. Lett. 130 (2023)

Beam spin asymmetry for DVCS on the proton



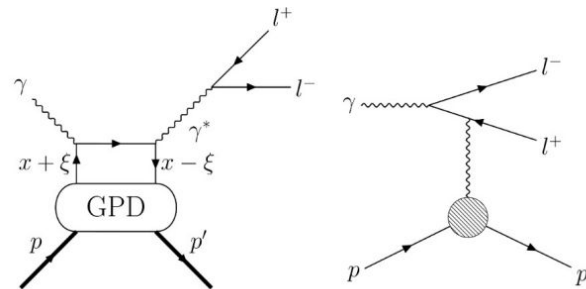
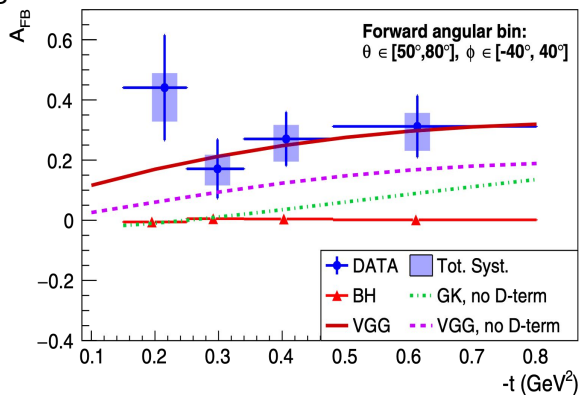
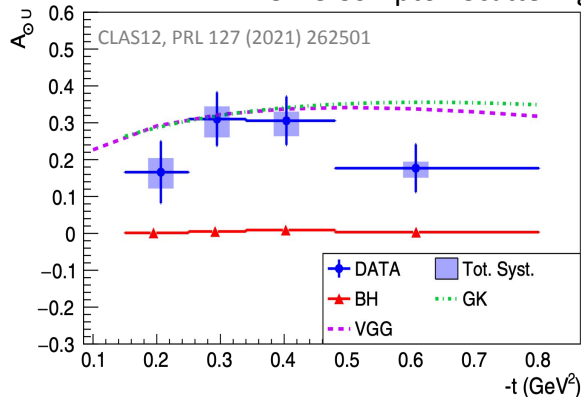
Beam-spin asymmetries in the extended valence region

- Many kinematics never covered before
- In previously measured kinematics, the new data are shown to be in good agreement with existing data and improve the precision of GPD fits
- Sensitivity to $\text{Im } \mathcal{H}$, the imaginary part of the CFF
- corresponding to the GPD H

First-time measurement of nDVCS with detection of the active neutron in progress

DVCS AND TCS AT CLAS12

Timelike Compton Scattering: time reversal to DVCS



(Timelike) Compton Scattering is the time reversal process of DVCS and allows us to test the universality of GPDs.

Photon polarization asymmetry

- Sensitive to $\text{Im}(\text{CFF})$
- Comparison to DVCS allows to test the universality of GPDs - especially the imaginary part of H

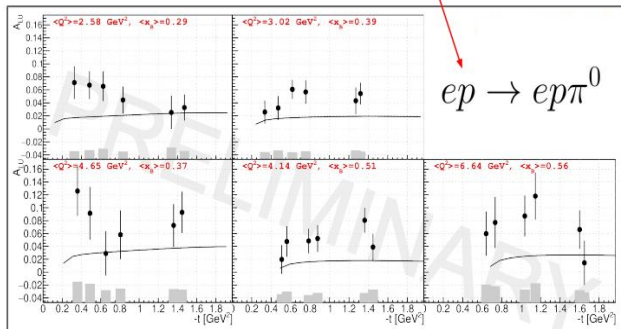
Forward-backward asymmetry

- Real part of the CFF and nucleon D-term
- Relates to mechanical properties of the nucleon (quark pressure distribution)

HARD EXCLUSIVE MESON PRODUCTION

π^+/π^0 beam spin asymmetries

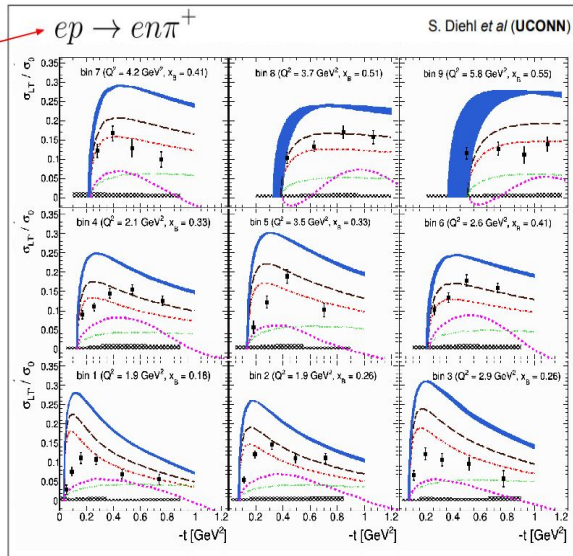
$$\sigma_{LT'} = \xi \sqrt{1 - \xi^2} \frac{\sqrt{-t'}}{2m} \times \text{Im} \left[\langle H_T \rangle^* \langle \bar{E} \rangle + \langle \bar{E}_T \rangle^* \langle \bar{H} \rangle \right]$$



A. Kim, CLAS12 Preliminary, APCTP 22

$ep \rightarrow ep\pi^0$

CLAS12, PLB 839, 137761 (2023)



S. Diehl et al (UCONN)

$$\frac{d^2\sigma_{\gamma^*p}^{\leftrightarrow}}{dt d\phi} = \frac{1}{2\pi} \left[\frac{d\sigma_T}{dt} + \epsilon \frac{d\sigma_L}{dt} + \epsilon \cos(2\phi) \frac{d\sigma_{TT}}{dt} + \sqrt{\epsilon(1+\epsilon)} \cos\phi \frac{d\sigma_{LT}}{dt} \mp |P_L| \sqrt{\epsilon(1-\epsilon)} \sin\phi \frac{d\sigma'_{LT}}{dt} \right]$$

$$\sqrt{\epsilon(1+\epsilon)} \cos\phi \frac{d\sigma_{LT}}{dt} \mp |P_L| \sqrt{\epsilon(1-\epsilon)} \sin\phi \frac{d\sigma'_{LT}}{dt}$$

	Meson	Flavor
$\mathcal{H}_T, \mathcal{E}_T$	π^+	$\Delta u - \Delta d$
	π^0	$2\Delta u + \Delta d$
	η	$2\Delta u - \Delta d + 2\Delta s$
$\mathcal{H}_L, \mathcal{E}_L$	ρ^+	$u - d$
	ρ^0	$2u + d$
	ω	$2u - d$
	ϕ	g

- DVMP offers access to the chiral-odd GPDs with separate pseudoscalar and vector meson measurements providing information on the flavor dependence.
- Chiral odd GPDs provide access to information on proton anomalous tensor magnetic moment, proton tensor charge and more.

Summary

- The CLAS12 facility at JLab offers an exceptional platform for conducting studies that are sensitive to nucleonic structure. This is primarily attributed to its impressive luminosity and comprehensive 4π coverage.
- Within the initial years of operation, CLAS12 has released several publications based on unpolarized H_2 data. Notably, many these publications introduced groundbreaking measurements for the first time.
- As we transition into the second phase of operations, we anticipate an exciting array of diverse measurements. This phase will encompass various aspects such as asymmetries, cross sections, differing energy levels, and a wide range of target materials and polarizations.

Backup

Longitudinal Spin Structure

- Decades of studies in **Deep Inelastic Scattering**, as well as **Semi-Inclusive Deep Inelastic Scattering** and **proton-proton** collisions
- **Polarized DIS cross section** studied at **SLAC, CERN, DESY, JLab** encodes information about **helicity structure of quarks** inside the proton (double spin asymmetries)

$$\frac{d^2\sigma_{LL}(x, Q^2)}{dx dQ^2} = \frac{8\pi\alpha^2 y}{Q^4} \left[\left(1 - \frac{y}{2} - \frac{y^2}{4}\gamma^2\right) g_1(x, Q^2) - \frac{y}{2}\gamma^2 g_2(x, Q^2) \right]$$

$$\nu = E - E'$$

$$y = \nu/E, \quad \gamma^2 = Q^2/\nu^2$$

$$g_1(x) = \frac{1}{2} \sum_q e_q^2 \Delta q(x)$$

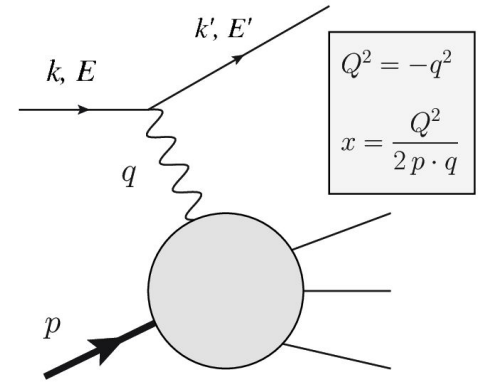
In (LO QCD) Quark Parton Model

Quark helicity distribution

Experimental access through double spin asymmetries

$$A_{\parallel} = \frac{\sigma_{LL}}{\sigma_{UU}} = \frac{1}{P_B P_z} \cdot \frac{\sigma_{\leftarrow\leftarrow}^{\rightarrow} - \sigma_{\leftarrow\rightarrow}^{\rightarrow}}{\sigma_{\leftarrow\leftarrow}^{\rightarrow} + \sigma_{\leftarrow\rightarrow}^{\rightarrow}} = D(1 + \eta\gamma) A_1$$

$$A_1 = \frac{g_1}{F_1}$$



D - Depolarization factor
 η - kinematic factor
 A_1 - photon-nucleon asymmetry

Longitudinal Spin Structure

- Decades of studies in **Deep Inelastic Scattering**, as well as **Semi-Inclusive Deep Inelastic Scattering** and **proton-proton** collisions
- **Semi-Inclusive Deep Inelastic Scattering** with charged pions and kaons adds **sensitivity to flavor-separated quark helicities** via the fragmentation functions $D_q^h(z, Q^2)$
 - valence parton content of h relates to the fragmenting parton flavor, particularly at high z
 z - fractional energy of the final-state hadron $z = E^h/\nu$

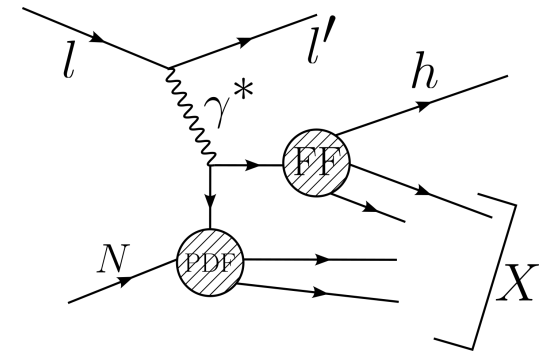
Photon-nucleon asymmetry for SIDIS

$$A_1^h = \frac{\sigma_{1/2}^h - \sigma_{3/2}^h}{\sigma_{1/2}^h + \sigma_{3/2}^h} \xrightarrow{\text{LO}} \frac{d^3 \sigma_{1/2(3/2)}^h}{dx dQ^2 dz} \propto \sum_q e_q^2 q^{+(-)}(x, Q^2) D_q^h(z, Q^2)$$

$$A_1^h(x, Q^2, z) = \frac{\sum_q e_q^2 \Delta q(x, Q^2) D_q^h(z, Q^2)}{\sum_{q'} e_{q'}^2 q'(x, Q^2) D_{q'}^h(z, Q^2)}$$

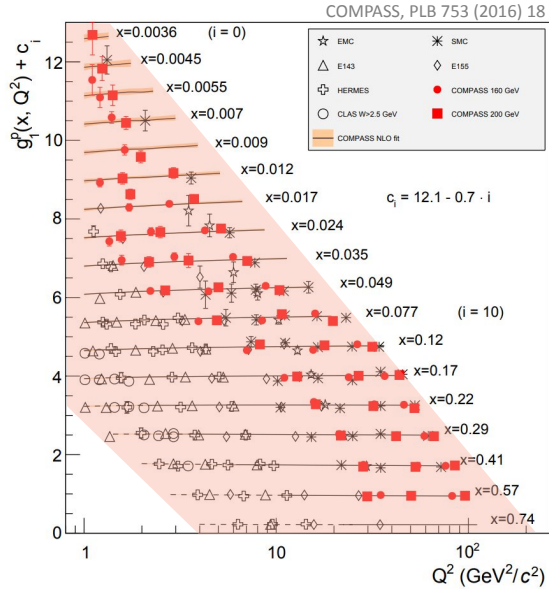
Experimental access through double spin asymmetries (analogous to DIS)

- Sensitivity to sea quarks at low x from $A_1^{\pi^-}(\Delta\bar{u})$, $A_1^{\pi^+}(\Delta\bar{d})$, $A_1^K(\Delta s)$

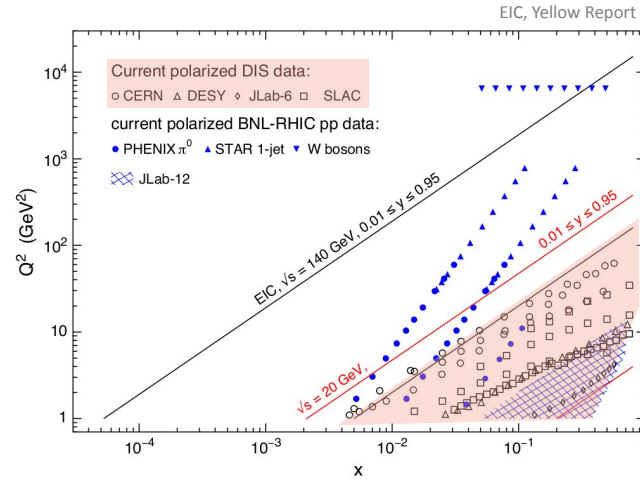
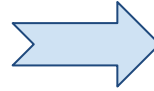


$$\sigma^{\text{SIDIS}} = \sigma^* \otimes \text{PDF} \otimes \text{FF}$$

Longitudinal Spin Structure - Where Are We Going?



Current DIS Data:
Down to $x \approx 0.005$
 $Q^2 \approx 1\text{-}100 \text{ GeV}^2$



EIC:

Down to $x \approx 10^{-4}$
 $Q^2 \approx 1\text{-}10^3 \text{ GeV}^2$!

- Access to gluon spin through g_1 scaling violation
- different \sqrt{s} settings to maximize kinematic coverage